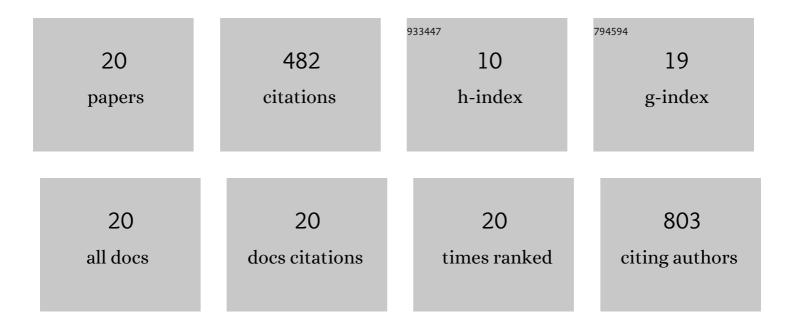


List of Publications by Year in descending order

Source: https://exaly.com/author-pdf/7830567/publications.pdf Version: 2024-02-01



#	Article	IF	CITATIONS
1	Magnetic-NIR Persistent Luminescent Dual-Modal ZGOCS@MSNs@Gd ₂ O ₃ Core–Shell Nanoprobes For In Vivo Imaging. Chemistry of Materials, 2017, 29, 3938-3946.	6.7	113
2	Chemical Transformation of Lead Halide Perovskite into Insoluble, Less Cytotoxic, and Brightly Luminescent CsPbBr ₃ /CsPb ₂ Br ₅ Composite Nanocrystals for Cell Imaging. ACS Applied Materials & Interfaces, 2019, 11, 24241-24246.	8.0	81
3	Spatiotemporal control of CRISPR/Cas9 gene editing. Signal Transduction and Targeted Therapy, 2021, 6, 238.	17.1	73
4	⁶⁸ Ga-Labeled Magnetic-NIR Persistent Luminescent Hybrid Mesoporous Nanoparticles for Multimodal Imaging-Guided Chemotherapy and Photodynamic Therapy. ACS Applied Materials & Interfaces, 2021, 13, 9667-9680.	8.0	37
5	Ultralong tumor retention of theranostic nanoparticles with short peptide-enabled active tumor homing. Materials Horizons, 2019, 6, 1845-1853.	12.2	27
6	A Honeycombâ€Like Bismuth/Manganese Oxide Nanoparticle with Mutual Reinforcement of Internal and External Response for Tripleâ€Negative Breast Cancer Targeted Therapy. Advanced Healthcare Materials, 2021, 10, e2100518.	7.6	25
7	Semi-quantitative evaluation of salivary gland function in Sjögren's syndrome using salivary gland scintigraphy. Clinical Rheumatology, 2012, 31, 1699-1705.	2.2	20
8	Bladder Cancer Photodynamic Therapeutic Agent with Offâ€On Magnetic Resonance Imaging Enhancement. Advanced Therapeutics, 2019, 2, 1900068.	3.2	19
9	The role of 99mTc-MIBI SPECT/CT in patients with secondary hyperparathyroidism: comparison with 99mTc-MIBI planar scintigraphy and ultrasonography. BMC Medical Imaging, 2020, 20, 115.	2.7	14
10	Overexpression of ribosomal L1 domain containing 1 is associated with an aggressive phenotype and a poor prognosis in patients with prostate cancer. Oncology Letters, 2016, 11, 2839-2844.	1.8	13
11	Radioiodine remnant ablation in papillary thyroid microcarcinoma. Nuclear Medicine Communications, 2019, 40, 711-719.	1.1	11
12	Semi-automatic evaluation of baseline whole-body tumor burden as an imaging biomarker of 68Ga-PSMA-11 PET/CT in newly diagnosed prostate cancer. Abdominal Radiology, 2020, 45, 4202-4213.	2.1	10
13	In Vivo MR Imaging of Dual MRI Reporter Genes and Deltex-1 Gene-modified Human Mesenchymal Stem Cells in the Treatment of Closed Penile Fracture. Molecular Imaging and Biology, 2018, 20, 417-427.	2.6	9
14	Brain MRI findings in acute hepatic encephalopathy in liver transplant recipients. Acta Neurologica Belgica, 2018, 118, 251-258.	1.1	8
15	<i>In Vivo</i> Assessment of Neurodegeneration in Type C Niemann-Pick Disease by IDEAL-IQ. Korean Journal of Radiology, 2018, 19, 93.	3.4	7
16	Multiple metastases in a novel LNCaP model of human prostate cancer. Oncology Reports, 2013, 30, 615-622.	2.6	6
17	Postoperative radioiodine therapy impact on survival in poorly differentiated thyroid carcinoma: a population-based study. Nuclear Medicine Communications, 2022, 43, 145-151.	1.1	5
18	Clinical and Contrast-enhanced Ultrasound Characteristics of Epithelioid and Classic Hepatic Angiomyolipoma: Comparison With Alpha-fetoprotein–negative Hepatocellular Carcinoma. Ultrasound in Medicine and Biology, 2021, 47, 446-453.	1.5	2

Ju Jiao

#	Article	IF	CITATIONS
19	18F-FDG PET/CT of Hepatosplenic Actinomycosis After Laparoscopic Cystojejunostomy for Pancreatic Pseudocyst. Clinical Nuclear Medicine, 2021, 46, e224-e225.	1.3	2
20	Diffuse Metastases in Bilateral Penile Corpus Cavernosum From Renal Cancer Diagnosed by 18F-FDG PET/CT. Clinical Nuclear Medicine, 2020, 45, 451-452.	1.3	0